

# Active Learning Using Aggregated Acquisition Functions: Accuracy and Sustainability Analysis

Cédric Jung, Shirin Salehi, Member, IEEE, and Anke Schmeink, Senior Member, IEEE

**Abstract**—Active learning (AL) is a machine learning (ML) approach that strategically selects the most informative samples for annotation during training, aiming to minimize annotation costs. This strategy not only reduces labeling expenses but also results in energy savings during neural network training, thereby enhancing both data and energy efficiency. In this paper, we implement and evaluate various state-of-the-art acquisition functions, analyzing their accuracy and computational costs, while discussing the advantages and disadvantages of each method. Our findings reveal that representativity-based acquisition functions effectively explore the dataset but do not prioritize boundary decisions, whereas uncertainty-based acquisition functions focus on refining boundary decisions already identified by the neural network. This trade-off is known as the exploration-exploitation dilemma. To address this dilemma, we introduce six aggregation structures: series, parallel, hybrid, adaptive feedback, random exploration, and annealing exploration. Our aggregated acquisition functions alleviate common AL pathologies such as batch mode inefficiency and the cold start problem. Additionally, we focus on balancing accuracy and energy consumption, contributing to the development of more sustainable, energy-aware artificial intelligence (AI). We evaluate our proposed structures on various models and datasets. Our results demonstrate the potential of these structures to reduce computational costs while maintaining or even improving accuracy. Innovative aggregation approaches, such as alternating between acquisition functions such as BALD and BADGE, have shown robust results. Sequentially running functions like  $K$ -Centers followed by BALD has achieved the same performance goals with up to 12% fewer samples, while reducing the acquisition cost by almost half.

**Index Terms**—Active learning, data-efficiency, energy efficiency, aggregated acquisition functions, exploration-exploitation dilemma, sustainability.

## I. Introduction

THE active learning (AL) framework in machine learning (ML) involves actively selecting and labeling training data to enhance model performance. The main objective is to reduce costs associated with obtaining labeled data by strategically choosing the most informative instances for annotation. In today's machine learning

This work was supported by the Federal Ministry of Education and Research (BMBF, Germany) as part of NeuroSys: Impulse durch Anwendungen (Projekt D) under Grant 03ZU1106DA.

S. Salehi and A. Schmeink are with the Chair of Information Theory and Data Analytics (INDA), RWTH Aachen University, 52074 Aachen, Germany (e-mail: shirin.salehi@inda.rwth-aachen.de; anke.schmeink@inda.rwth-aachen.de)

C. Jung was with the Chair of Information Theory and Data Analytics (INDA), RWTH Aachen University, 52074 Aachen, Germany. He is now with the Automation and Control Institute, Technische Universität Wien (TUW), 1040 Vienna, Austria, and also with the AIT Austrian Institute of Technology GmbH, 1210 Vienna, Austria (e-mail: jung@acin.tuwien.ac.at)

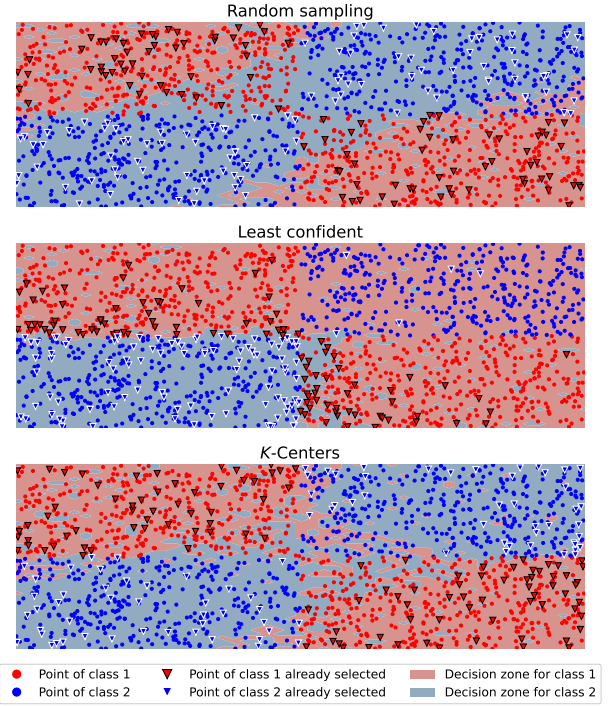


Fig. 1. Illustration of selected samples and current decision boundary of grid toy dataset at acquisition step 20 with a budget  $b = 10$  using a simple fully connected network (FCN) with the following structure: dense-relu-dropout-dense-relu-dense-softmax.

landscape, active learning stands out as particularly pertinent, especially in cases where there is an abundance of unlabeled data that is easily accessible while the labeling process is difficult, time-consuming, or expensive [1].

In recent years, the field of artificial intelligence (AI) has seen remarkable progress due to the exponential increase in computational power and the availability of large-scale datasets. This progress has resulted in the development of complex models and innovative applications. However, these models require substantial amounts of energy, leading to increased greenhouse gas emissions and a larger carbon footprint within the AI industry [2], [3]. To address these issues, the concept of green AI has emerged [4], emphasizing energy efficiency and sustainability alongside traditional metrics like accuracy. Furthermore, the training of these models necessitates processing vast amounts of data [5], which in turn consumes substantial energy and contributes significantly to the carbon footprint. AL shows promising potential to enhance both data and energy efficiency [6], [7], [8].

In active learning, an acquisition function is employed to pick out samples from a vast pool of unlabeled data. This decision is guided by the current iteration of the neural network, which has been trained with samples selected during previous acquisition rounds. Diverse acquisition functions have been developed following different paradigms or implementation principles. Each of these approaches has its own set of strengths and weaknesses, exhibiting varied behavior depending on the datasets and model architecture utilized. Consequently, one function may over-perform the other, or not, depending on these factors. Therefore, there is no one-fits-all solution for AL.

In AL one wants to minimize the number of data to request. The challenge lies in choosing between exploring new, potentially informative data points and exploiting the current model's knowledge to improve performance. This is called the exploration-exploitation dilemma [9], [10], [11]. Exploitation involves selecting samples that the current model is uncertain about or likely to be misclassified, aiming to refine the model's decision boundaries in areas of uncertainty. In contrast, exploration involves choosing samples that are different from those already labeled, potentially introducing new concepts or classes that the model has not encountered before. In summary, the exploration strategy aims to cover regions of the input space, while the exploitation strategy looks to refine the boundary decision.

Balancing exploration and exploitation in AL is crucial to maximize the efficiency of the labeling process. Over-reliance on exploitation may lead to the model being stuck in local optima or missing out on valuable insights from unexplored regions of the data space. In contrast, excessive exploration can result in labeling redundant or less informative data points, wasting annotation resources. The exploration-exploitation dilemma is illustrated in Fig. 1. In this figure, the grid toy dataset is used to show the selection of samples according to random sampling, least confident, and  $K$ -Centers, respectively. The decision zones depict the results of the model evaluation trained on the samples selected for 20 acquisition rounds with a budget of  $b = 10$ . One can clearly see that least confident, an uncertainty-based acquisition function, is selecting samples at the boundary decisions of the bottom-left part. However, it fails to discover the two other boundary decisions, resulting in poor accuracy with such a simple problem (77% of accuracy). On the other hand, the coresets-inspired acquisition function  $K$ -Centers succeeds in covering the dataset, but has a fuzzy boundary decision and achieves higher performance (94% of accuracy) compared to random sampling (86% of accuracy). With this example, one can clearly see the advantages and disadvantages of acquisition paradigms.

In order to improve the performance of AL acquisition functions, one can consider combining different acquisition functions instead of conceiving other sophisticated acquisition functions that can only be effective in some edge cases. Intuitively, the combination of methods can enable us to leverage the advantages of some methods while mitigating

the limitations of others. In particular, the contributions of this paper can be summarized as follows:

- Evaluate basic and state of the art baseline acquisition functions in terms of accuracy and energy consumption.
- Proposing various structures to aggregate multiple acquisition functions, aiming to enhance accuracy while keeping computational costs moderate by strategically combining acquisition functions with different characteristics.
- Assess the performance of the proposed approaches across a variety of model structures and datasets, in order to evaluate the generalization and robustness of the proposed approaches.

The rest of this paper is organized as follows: We begin by reviewing related works in Section II, providing context and background information on active learning. In Section III, we delve into previous works on aggregating acquisition functions. Section IV presents more detail on proposed structures for aggregating acquisition functions. Finally, these structures are evaluated in Section V, showing the practical applications of such structures, before concluding the paper in Section VI.

## II. Active Learning

### A. Problem settings

Active learning, also referred to as query learning, strives to enhance a model's performance by minimizing the number of labeled samples needed. Its core concept is straightforward: Different samples in a dataset carry varying degrees of importance for updating the current model, allowing us to pinpoint the most influential examples for training. For effective scaling of machine learning to handle larger problems or more frequent use, it is essential to grasp theoretically and measure the significance of different data points during training and optimization. This enables us to discern valuable samples that contribute meaningfully to the learning process while excluding redundant or uninformative ones confidently.

AL typically starts with a small training set to train the model. The model then predicts outcomes for unlabeled data, selecting samples that have the greatest potential to improve the model's accuracy are selected for manual labeling. Labeled samples are added to the training set, and this process repeats until the desired accuracy or labeling budget is reached.

In the case of pool-based AL and considering the classification tasks, we can define the AL problem as follows. The whole dataset at first presents a small labeled dataset part named  $\mathcal{D}_L = \{(x_j, y_j)\}_{j=1}^M$  and a larger unlabeled dataset part named  $\mathcal{D}_U = \{x_i\}_{i=1}^N$  where  $M \ll N$ ,  $y_i \in \{0, 1\}$  is the class label of  $x_i$  for binary classification, or  $y_i \in \{1, \dots, C\}$  for multi-class classification. The process involves selecting instances from the unlabeled dataset  $\mathcal{D}_U$  in a greedy manner, guided by a set of informativeness metrics. These metrics are encapsulated by what is known as an "acquisition

function". The acquisition function helps to determine the most informative or valuable data points for labeling, facilitating an efficient and effective AL process. Thus, in each iteration  $t$ , we select a sample from  $\mathcal{D}_{\mathcal{U}}$  based on the learned model  $\mathcal{M}$  and an acquisition function  $\alpha(x, \mathcal{M})$ , and query their labels from the oracle. Data samples can be selected according to their acquisition score by  $x^* = \operatorname{argmax}_{x \in \mathcal{D}_{\mathcal{U}}} \alpha(x, \mathcal{M})$ . In general to reduce computational costs, a pool  $\mathcal{D}_{\text{pool}}$  is drawn from the unlabeled dataset  $\mathcal{D}_{\mathcal{U}}$ , on which the acquisition function will be computed:  $x^* = \operatorname{argmax}_{x \in \mathcal{D}_{\text{pool}}} \alpha(x, \mathcal{M})$ .

## B. Batch mode active learning (BMAL)

Although historical methods acquire one sample at a time [12], [13], [14], since deep neural networks (DNNs) are computationally heavy, training a new model with a single training sample is highly impractical. Therefore, methods are developed in order to acquire multiple training samples at a time. Moreover, even if it was computationally feasible, a single sample would not have a significant impact statistically on the model given the optimization process. Therefore, in batch mode active learning (BMAL), in each iteration  $t$ , we select a batch of samples  $\mathcal{D}_t$  with batch size  $b = |\mathcal{D}_t|$  from  $\mathcal{D}_{\mathcal{U}}$  instead of only one sample. Data samples can be selected according to their acquisition score by  $\mathcal{D}_t^* = \operatorname{argmax}_{x \in \mathcal{D}_{\text{pool}}} \alpha(x, \mathcal{M})$ , where the superscript  $b$  indicates selection of the top  $b$  points. This is known as Top- $K$  in the literature. However, this can be inefficient if multiple similar samples are selected, leading to redundant information. Acquisition function designs must typically take into account typically three criteria: informativeness, representativeness, and diversity.

- 1) Informativeness or Uncertainty is a function  $\tau(x)$  that quantifies how much a classifier is expected to benefit from selecting a specific sample  $x$ . There are several categories of informativeness functions. One can divide such functions into data-based informativeness, which only relies on  $\mathcal{D}_{\mathcal{L}}$  and  $\mathcal{D}_{\mathcal{U}}$ , and model-based informativeness, which only relies on the trained classifier.
- 2) Diversity is a function  $div(B)$  that only makes sense when applied to a batch  $B = \{x_i\}_{i=1}^b$ , contrary to the othermentioned criteria. Intuitively, the batch is the most diverse when the samples are the most dissimilar. From an AL perspective having a high diversity batch is good as this will prevent having huge information overlap. Diversity can be achieved explicitly or implicitly.
- 3) Representativeness or representativity is a function  $rep(x)$  that quantifies how well a sample represents the data set. However, there are multiple interpretations and implementations of representativeness. One can consider the density of samples which can be determined by  $k$ -NN-density measure as proposed by [15], where the density of a batch is given by the

average distance between the  $k$  most similar samples within  $\mathcal{D}_{\text{pool}}$ .

## C. Aquisition functions: an overview

As mentioned earlier, an acquisition function or query strategy is utilized by the model to evaluate its uncertainty or to pinpoint instances that are likely to yield the most valuable information. Several query selection strategies are introduced below.

1) Uncertainty sampling: The uncertainty sampling approach is the most frequently used paradigm [12]. An acquisition function based on this framework queries the data samples about which the model  $\mathcal{M}$  is most uncertain, given the conditional distribution  $P(y|x, \omega)$ , where  $\omega$  denotes the model parameters. This kind of acquisition strategy leads to selecting samples near the decision boundaries. A widely adopted uncertainty sampling strategy, Max Entropy or more concisely Entropy, employs Shannon entropy [16], as a measure of uncertainty:

$$\begin{aligned} x_{\mathbb{H}}^* &= \operatorname{argmax}_{x \in \mathcal{D}_{\text{pool}}} - \sum_i P(y_i|x, \omega) \log P(y_i|x, \omega) \\ &= \operatorname{argmax}_{x \in \mathcal{D}_{\text{pool}}} \mathbb{H}(y|x, \omega), \end{aligned} \quad (1)$$

where  $\mathbb{H}$  is the entropy function. Simpler uncertainty acquisition functions are also used, namely Least confident, also named Variation ratio, which selects the samples with the least confidence:

$$x_{LC}^* = \operatorname{argmax}_{x \in \mathcal{D}_{\text{pool}}} 1 - P(\hat{y}|x, \omega), \quad (2)$$

where  $\hat{y} = \operatorname{argmax}_y P(y|x, \omega)$  indicates the class label with the highest posterior probability under the model  $\mathcal{M}$  with its associated parameters  $\omega$ . Another acquisition function, Margin sampling, takes into account the entire label distribution rather than just the most probable label:

$$x_{MS}^* = \operatorname{argmin}_{x \in \mathcal{D}_{\text{pool}}} P(\hat{y}_1|x, \omega) - P(\hat{y}_2|x, \omega), \quad (3)$$

where  $\hat{y}_1$  and  $\hat{y}_2$  represent the top two class labels with the highest probabilities predicted by the model, respectively. Another strategy, Mean STD [17], selects the samples that maximize the average standard deviation over all possible classes:

$$x_{MeanSTD}^* = \operatorname{argmax}_{x \in \mathcal{D}_{\text{pool}}} \frac{1}{C} \sum_i \sigma_i, \quad (4)$$

$$\sigma_i = \sqrt{\mathbb{E}_{q(\omega)}[P(y_i|x, \omega)^2] - \mathbb{E}_{q(\omega)}[P(y_i|x, \omega)]^2}, \quad (5)$$

where  $C$  is the number of classes and  $q(\omega)$  is the dropout distribution.

2) BALD: Bayesian active learning by disagreement (BALD) [14] defines an acquisition function based on epistemic uncertainty. Through BALD the samples are selected in such a way that produces disagreeing prediction with high certainty, i.e. stochastic forward passes would have the highest probability to assign the samples to different classes. Specifically, it uses the mutual information

(MI) between the unknown output and model parameters as a measure of disagreement:

$$\mathbb{I}(y; \omega|x, \mathcal{D}_L) = \mathbb{H}(y|x, \mathcal{D}_L) - \mathbb{E}_{\omega \sim p(\omega|\mathcal{D}_L)} [\mathbb{H}(y|x, \omega)]. \quad (6)$$

BALD tries to maximize the mutual information or more explicitly the information gained about the model parameters,  $\mathbb{I}(y; \omega|x, \mathcal{D}_L)$ , between predictions and model posterior:

$$x_{BALD}^* = \operatorname{argmax}_{x \in \mathcal{D}_{pool}} \mathbb{I}(y; \omega|x, \mathcal{D}_L). \quad (7)$$

A computationally cheaper way to avoid computing the mutual information gain was found by [18], while it is still capable of mitigating information overlap. The authors introduce a weighted importance sampling across  $\mathcal{D}_{pool}$  taking the individual scores given by BALD as input. They introduce a class of acquisition functions called stochastic acquisition function which includes PowerBALD.

3) Greedy  $K$ -Centers: Introduced in [19], Greedy  $K$ -Centers or simply  $K$ -Centers is a core-set inspired acquisition function which allows to enforce diversity of selected samples on the unlabeled batch. The core-set selection problem is to select a subset of the whole dataset so that the model trained on this subset performs as closely as possible to the model trained on the entire dataset. This method does not include the notion of informativeness directly, but instead selects instances that best cover the dataset by maximizing the minimal distance to the labeled set  $\mathcal{D}_L$  on the learned feature space (last hidden layer of the neural network).

4) BADGE: The state-of-the-art acquisition function Batch Active Learning by Diverse Gradient Embeddings (BADGE), has been introduced recently in [20]. It selects samples by first computing the last-layer gradient  $g_x = \nabla l(x, y = \hat{y}, \omega^L)$  (gradient embedding), obtained if the most likely label according to the model,  $\hat{y}$ , were observed. Here  $\omega^L$  refers to the parameters of the last hidden layer. It then uses  $k$ -Means++ to select  $b$  samples [21]. The use of  $k$ -Means++ is motivated by the fact that it is a computationally efficient approximation of Determinantal Point Process (DPP) sampling.

The authors who originally proposed BADGE later introduced Batch Active learning via Information matrices (BAIT), a more recent acquisition function that extensively leverages Fisher Information (FI) and is designed for use in a BMAL framework [22]. Considering the negative log-likelihood  $l(x, y, \omega) = -\log p(y|x; \omega)$ , FI can be written as  $\mathcal{I}_x(\omega) = \mathbb{E}_{p(y|x; \omega)} [\nabla_\omega^2 l(x, y, \omega)]$ . BAIT selects batches by minimizing a Fisher information-based objective:

$$\operatorname{argmin}_{S \subseteq \mathcal{D}_{pool}, |S| \leq b} \operatorname{tr} \left( \left( \sum_{x \in S} \mathcal{I}_x(\omega) \right)^{-1} \mathcal{I}_{\mathcal{U}}(\omega) \right) \quad (8)$$

with  $\mathcal{I}_{\mathcal{U}}(\omega) = \sum_{x \in \mathcal{D}_{pool}} \mathcal{I}_x(\omega)$ . The authors claim that BADGE is in fact an approximation of BAIT, resulting in better result in terms of the number of samples required. BAIT has the advantage over BALD to consider all the

possible labels  $y$ , while BADGE only considers the most probable label. However, BADGE is  $C$  times faster than BAIT, where  $C$  is the number of classes.

5) Submodularity-based acquisition function: Submodular functions inherently represent concepts of information, diversity, and coverage in various applications [23]. Additionally, they can be optimized effectively using remarkably straightforward algorithms. A greedy algorithm [24] guarantees that the cardinality constrained submodular maximization problem can be approximated to a factor of  $1 - \frac{1}{e}$ . It is therefore natural that they have been used in AL [25]. The discussion below will present only two of these functions.

a) Facility location: Facility location (FL) function [26] aims to represent the data by identifying a subset of representative elements. This submodular function goal is to have the most representative subset. The idea is similar to  $k$ -medoids clustering. FL is solved by acquiring in a greedy manner the samples that have the maximum similarity to the groundset:

$$\begin{aligned} \mathcal{D}_t^* &= \operatorname{argmax}_{\mathcal{D}_t \subseteq \mathcal{D}_{pool}} \alpha_{FL}(\mathcal{D}_t, \mathcal{D}_L, \mathcal{M}) \\ &= \operatorname{argmax}_{\mathcal{D}_t \subseteq \mathcal{D}_{pool}} \sum_{x_i \in \mathcal{D}_{pool}} \max_{x_j \in \mathcal{D}_t} s(x_i, x_j) \end{aligned} \quad (9)$$

where  $s(x_i, x_j)$  denotes the similarity between  $x_i$  and  $x_j$ .

b) Disparity min: In contrast to FL, disparity functions are diversity-based functions that strive to acquire a diverse set of samples, with the objective of minimizing similarity among elements in the selected subset by maximizing the minimum distance between pairs. The minimum disparity function (disparity min) [27] can be expressed as follows:

$$\begin{aligned} \mathcal{D}_t^* &= \operatorname{argmax}_{\mathcal{D}_t \subseteq \mathcal{D}_{pool}} \alpha_{Disparity\ min}(\mathcal{D}_t, \mathcal{D}_L, \mathcal{M}) \\ &= \operatorname{argmax}_{\mathcal{D}_t \subseteq \mathcal{D}_{pool}} \min_{x_i, x_j \in \mathcal{D}_t} d(x_i, x_j) \end{aligned} \quad (10)$$

where  $d(x_i, x_j)$  denotes the distance between  $x_i$  and  $x_j$ . This function is not submodular, but according to [27] it can also be optimized via a greedy algorithm.

### III. Related works

The concept of aggregating acquisition functions in a series structure, as outlined in this work, is not entirely novel. Englhardt et al. [28] explored this in a one-class problem context. Similarly, Wei et al. [25] introduced the Filtered Active Submodular Selection (FASS) framework. Although they did not explicitly define a series structure, their multistage framework—initially selecting  $\kappa b$  samples based on uncertainty scores and the most likely label, followed by the application of a submodular function to select the final  $b$  samples—aligns closely with this concept.

The concept of information density weighting, as discussed by Settles et al. [29], integrates diversity and uncertainty. The idea is to counter-weight the uncertainty in the selection of samples to also take into account the most representative points of the data distribution. This

means that the acquisition function should also select samples in the dense regions of the data distribution. The information density acquisition function is introduced by [29] as follows and is composed of two parts:

$$x_{\text{ID}}^* = \underset{x \in \mathcal{D}_{\text{pool}}}{\text{argmax}} \phi(x) \times \left( \frac{1}{|\mathcal{D}_{\text{pool}}| - 1} \sum_{z \in \mathcal{D}_{\text{pool}} \setminus \{x\}} \text{sim}(x, z) \right)^\beta, \quad (11)$$

where  $\phi(x)$  represents the informativeness of  $x$  according to a first acquisition function (uncertainty-based for example), while the second term is the average similarity to all other samples from the data distribution  $\mathcal{D}_{\text{pool}}$ . The hyperparameter  $\beta$  allows one to balance the importance of the two terms. This method ensures that uncertain samples with redundant information are not repeatedly selected, thereby improving the efficiency of the active learning process. Authors in [30] also implemented such an approach leveraging support vector machine's (SVM) ability to compute distance.

Incorporating a clustering step, as suggested in [30] and [25], can enhance the selection of diverse samples, ensuring broad coverage of the feature space. The pre-clustering approach from Nguyen et al. [31] further refines this by dynamically adjusting cluster sizes to balance exploration and exploitation.

The diversity measure in uncertainty sampling, as explored by Yin et al. [9], addresses the exploitation-exploration dilemma. They define exploitation as selecting maximally uncertain and minimally redundant instances and exploration as selecting samples most diverse from the labeled set. Their formula  $I(S) = E(S) - \beta R(S)$  incorporates redundancy reduction directly into the acquisition process. Gu et al. [32] proposed a similar method using SVM and Gaussian kernel to compute similarity. Although this method does not involve deep learning, it focuses on minimizing redundancy while maximizing information gain.

Fixed combinations of acquisition functions, with pre-defined trade-off parameter  $\beta$ , have evolved into adaptive combinations where the trade-off parameter adjusts dynamically. Our feedback-driven method is inspired by this adaptive approach. However, it selects among different acquisition functions based on the feedback signal on acquisition rounds rather than on a fixed ratio over the entire acquisition process.

The feedback-driven acquisition functions have been studied in works such as Ebert and Ralf [33] and Cheng et al. [34]. Their approach weights the contribution of uncertainty-based and diversity-based acquisition functions using a dynamic trade-off ratio  $\beta(t)$ . They implemented a weighted sum of the ranks provided by two acquisition functions. This is similar to one of our proposed approaches called parallel-ranked. However, they use a single-sample selection at a time, which contrasts with our BMAL approach. Their approach uses the following equation for the acquisition round  $t$ :

$$\alpha_t(x_i, \mathcal{M}) = \beta(t)r(U(x_i)) + (1 - \beta(t))r(D(x_i)), \quad (12)$$

with  $r$  being the ranking function, and  $\beta(t)$  a trade-off ratio. A batch can be selected in a Top- $K$  manner:

$$\mathcal{D}_t^* = \underset{x \in \mathcal{D}_{\text{pool}}}{\text{argmin}} \alpha(x, \mathcal{M}) \quad (13)$$

Their method thus combines the disadvantages of parallel-ranking and Top- $K$  selection, while our approach provides feedback to choose between acquisition functions rather than a weighted rank combination, potentially reducing Top- $K$  selection pathologies within the combined acquisition functions.

Several studies have employed bandit approaches to balance exploration and exploitation in active learning in the same manner. For instance, Tran et al. [35] used Thompson sampling, Baram et al. [36] applied the EXP4 algorithm, and Hu et al. [37] explored similar methodologies. These approaches dynamically adjust the exploration-exploitation trade-off, striving for optimal sample selection under finite data constraints, acknowledging that even the best heuristics may fall short due to poor classifiers trained on limited data.

Recent work by Flesca et al. [38] is a meta-learning approach which computes importance scores based on criteria like direct similarity or leave-one-out distance and trains a regression model on pairs of labeled instances, each associated with an importance score. This approach aims to predict the most likely importance score for future acquisitions, enhancing the decision-making process in active learning. A recent work [10] introduced dynamic trade-offs in exploration and exploitation, emphasizing the need for iterative updates to the trade-off parameter as new data is queried. This contrasts with classical approaches that use a fixed trade-off parameter, highlighting the need for flexibility in active learning strategies.

#### IV. Proposed structures for aggregated acquisition functions

In this section, the proposed structures for aggregating acquisition functions are introduced, the motivation behind them is explained, and their expected pros and cons are discussed.

##### A. Parallel and parallel-ranked structures

In parallel and parallel-ranked structures, acquisition functions run in parallel, and then the results are combined.

1) Parallel-ranked: A straightforward approach is to sum the ranks provided by two acquisition functions and then select the Top- $K$  samples, as shown in Fig. 2. The combined acquisition function can thus be expressed as:

$$\alpha(x_i, \mathcal{M}) = r(\alpha_1(x_i, \mathcal{M})) + r(\alpha_2(x_i, \mathcal{M})), \quad (14)$$

with  $r$  the ranking function  $r : \mathbb{R} \rightarrow \{1, \dots, u\}$ ,  $r(F(x_i)) = m_i$ , where  $F(x_i) \leq F(x_j) \Leftrightarrow m_i \geq m_j$  with  $m \in \{1, \dots, u\}$

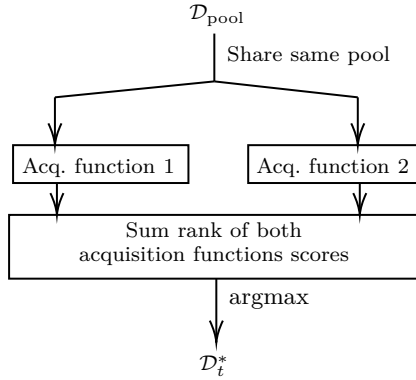


Fig. 2. Schema of parallel-ranked combination of two acquisition functions.

with  $F$  a real-valued function. A batch can be selected in a Top- $K$  manner:

$$D_t^* = \operatorname{argmin}_{x \in D_{\text{pool}}}^b \alpha(x, \mathcal{M}) \quad (15)$$

This approach, which we call parallel-ranked, has two drawbacks. Firstly, not all the acquisition functions give a score to samples (for example BADGE), which makes this structure infeasible. Secondly, scores sometimes cancel each other out. For instance, two acquisition functions can give midscores to a sample, and the sum of them would result in selecting the sample, while none of the acquisition functions considers this sample good enough for selection. This does not give automatically the best of two acquisition functions criteria and can even have lower performance than originally considered acquisition functions alone. Furthermore, it can intensify the pathologies of batch selection.

2) Parallel: Another approach is to run two acquisition functions in parallel on different subsets of the pool and then dedicate only a part of the budget  $b$  to the samples selected via each acquisition function. We call this structure parallel. This is done because running acquisition functions can be computationally expensive and as we cannot ensure that acquisition functions will not select the same samples, one considers them running only on a part of the pool  $D_{\text{pool}}$ . If two acquisition functions are considered to run in parallel, each will select a budget of  $\frac{1}{2}b$  from a pool of size  $\frac{1}{2}|D_{\text{pool}}|$ . This structure is illustrated in Fig. 3. Formally, this approach can be written as:

$$\begin{aligned} D_t^* &= \alpha(D_{\text{pool}}, b, \mathcal{M}) \\ &= \alpha_1\left(D_{\frac{|D_{\text{pool}}|}{2}}, \frac{b}{2}, \mathcal{M}\right) \cup \alpha_2\left(D_{\frac{|D_{\text{pool}}|}{2}}, \frac{b}{2}, \mathcal{M}\right). \end{aligned} \quad (16)$$

Here, the second argument denotes the batch size to be selected, and  $D_{\frac{|D_{\text{pool}}|}{2}}$  represents a split of the pool  $D_{\text{pool}}$  of cardinality  $\frac{|D_{\text{pool}}|}{2}$ .

## B. Series structure

In this approach, the acquisition functions are aggregated in a series manner. In the series structure, at least two acquisition functions are applied sequentially, each

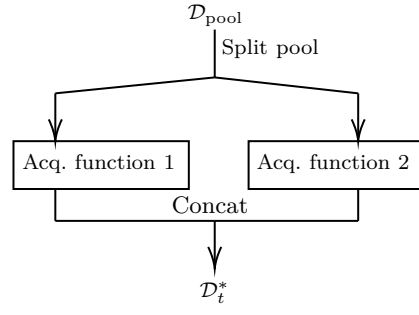


Fig. 3. Schema of the parallel combination of two acquisition functions. By ‘‘Concat’’ we refer to the concatenation of the elements of the selected batches into a single batch.

reducing the pool of data on which the next acquisition function will operate. This structure can be visualized as a sieve with multiple layers. In this framework, we define a subsample factor  $\kappa \geq 1$ , which determines the additional budget  $\kappa b$  allocated to the first acquisition function. This extra budget is progressively reduced at the next layer, ultimately converging to the final budget  $b$ . Given two acquisition functions  $\alpha_1$  and  $\alpha_2$ , a subsample factor  $\kappa \geq 1$  is applied. At acquisition step  $t$ :

$$\begin{aligned} D_{t,1}^* &= \alpha_1(D_{\text{pool}}, \kappa b, \mathcal{M}), \\ |\mathcal{D}_{t,1}^*| &= \kappa b, \\ D_t^* &= \alpha_2(\mathcal{D}_{t,1}^*, b, \mathcal{M}), \\ |\mathcal{D}_t^*| &= b, \end{aligned} \quad (17)$$

where the second argument denotes the batch size to be selected.

This structure has the advantage of reducing the pool for the second acquisition function. Generally,  $|\mathcal{D}_{\text{pool}}| \gg \kappa b$ , the cost of using this second acquisition function on top of the first is limited compared to running two acquisition functions on the whole pool. The series structure is detailed in algorithm Algorithm 1.

## C. Hybrid structure

Another way to combine the acquisition functions is to mix the parallel and series structures. This structure allows us to run two acquisition functions on the same pool like parallel-ranked, while having the knowledge of selected samples by the first one. The only restriction compared to the parallel structure is that one has to execute the functions one after another. This structure is proposed in order to improve the performance of the parallel structure. This structure can be written using recursive equations:

$$\begin{aligned} \mathcal{D}_{t,0}^* &= \emptyset, \\ \mathcal{D}_{t,1}^* &= \alpha_1(D_{\text{pool}}, b_1, \mathcal{M}), \\ \mathcal{D}_{t,2}^* &= \alpha_2(D_{\text{pool}} \setminus \mathcal{D}_{t,1}^*, b_2, \mathcal{M}), \\ \mathcal{D}_t^* &= \mathcal{D}_{t,1}^* \cup \mathcal{D}_{t,2}^*. \end{aligned} \quad (18)$$

with a total budget of  $b = b_1 + b_2$ . It can be seen that the hybrid structure is just the execution of several acquisition rounds with a total budget  $b$  without retraining the model  $\mathcal{M}$ , which is the costly part.

---

**Algorithm 1** Active learning with series structure

---

Input: Neural network  $\mathcal{M} = f(x; \omega)$   
 Input: Unlabeled dataset  $\mathcal{D}_{\mathcal{U}}$   
 Input: Initial number of samples  $M$ ,  
 Input: Total number of iterations  $T$   
 Input: Number of samples in a batch  $b$   
 Input: Acquisition functions list  $[\alpha^{(1)}, \alpha^{(2)}, \dots, \alpha^{(N_{\text{acq}})}]$   
     containing  $N_{\text{acq}}$  acquisition functions  
 Input: Subsample factor list  $[\kappa_1, \kappa_2, \dots, \kappa_{N_{\text{acq}}}]$  containing  
      $N_{\text{acq}}$  factors with  $\kappa_1 \geq \kappa_2 \geq \dots \geq \kappa_{N_{\text{acq}}} \geq 1$   
 1: Labeled dataset  $\mathcal{D}_{\mathcal{L}} \leftarrow M$  examples drawn randomly  
     from  $\mathcal{D}_{\mathcal{U}}$  together with queried labels.  
 2: Train an initial model  $\mathcal{M}_0$  on  $\mathcal{D}_{\mathcal{L}}$ .  
 3: for  $t = 1, \dots, T - 1$  do  
 4:     Draw  $\mathcal{D}_{\text{pool}}$  randomly from  $\mathcal{D}_{\mathcal{U}}$   
 5:      $\mathcal{D}_t^{*(0)} \leftarrow \mathcal{D}_{\text{pool}}$   
 6:     for  $i = 1, \dots, N_{\text{acq}}$  do  
 7:         Select  $b$  sample  $\mathcal{D}_t^{*(i)} \leftarrow \alpha^{(i)}(\mathcal{D}_t^{*(i-1)}, \kappa_i b, \mathcal{M}_t)$   
 8:     end for  
 9:      $\mathcal{D}_{\mathcal{U}} \leftarrow \mathcal{D}_{\mathcal{U}} \setminus \mathcal{D}_t^{*(N_{\text{acq}})}$   
 10:     $\mathcal{D}_{\mathcal{L}} \leftarrow \mathcal{D}_{\mathcal{L}} \cup \mathcal{D}_t^{*(N_{\text{acq}})}$   
 11:    Train a model  $\mathcal{M}_{t+1}$  on  $\mathcal{D}_{\mathcal{L}}$ .  
 12: end for  
 13: return Final model  $\mathcal{M}_T$ .

---

In the following subsections, we present selection mechanisms for switching between acquisition functions, including adaptive feedback, annealing, and random alternation. The computational cost of employing such a dual-strategy scheme is comparable to that of using a single acquisition function, since only one function is executed in each iteration. The only additional overhead stems from evaluating the selection mechanism itself, which is negligible relative to the overall training cost.

#### D. Adaptive feedback structure

A more sophisticated approach selects between acquisition functions based on a feedback signal. To choose the acquisition function  $\alpha_{t+1}$  for the next AL iteration  $t+1$ , we use the loss of the previous model  $\mathcal{M}_{t-1}$ —not the current model  $\mathcal{M}_t$ —evaluated on the current selected batch  $\mathcal{D}_t^*$ . Intuitively, this loss is a meaningful metric, as it reflects the model’s error on data it has not seen before. We refer to this method as adaptive feedback due to its similarity to a feedback control loop.

The key idea is to alternate between exploration-oriented acquisition functions (e.g.,  $K$ -Centers) and exploitation-oriented ones (e.g., BALD) depending on the observed behavior of the feedback metric. Exploration is favored when the model is still discovering new regions of the input space, while exploitation is triggered when uncertainty increases around decision boundaries. This strategy alleviates the cold-start problem in active learning and mitigates the tendency of uncertainty-based functions to focus only on poorly conditioned boundaries. The cost of using such a structure is the same as running

acquisition functions alone, as per iteration round, only one acquisition function is running, plus the cost of choosing the feedback. The additional cost, therefore, only depends on the feedback strategy.

In our implementation, the feedback metric is the previous model loss:

$$\ell_t = J(\mathcal{D}_t^*, \omega_{t-1}), \quad (19)$$

where  $J$  is the loss function and  $\omega_{t-1}$  are the parameters of  $\mathcal{M}_{t-1}$ . Since  $\ell_t$  tends to decrease over time due to empirical risk minimization, we normalize it over a sliding window of size  $n_{\text{window}}$ :

$$s_t = \frac{\ell_t - \min(\ell_{t-n_{\text{window}}:t})}{\max(\ell_{t-n_{\text{window}}:t}) - \min(\ell_{t-n_{\text{window}}:t})}. \quad (20)$$

Here  $s_t \in [0, 1]$  serves as a scaled reward, where higher values indicate that the selected batch was more challenging for the model. This idea was inspired by the client selection framework in federated learning proposed by [39], where clients are selected based on the larger local loss.

As a trade-off update rule, we maintain a trade-off parameter  $\beta_t \in [\epsilon, 1 - \epsilon]$  ( $\epsilon > 0$ ) controlling the exploration-exploitation choice:

$$\beta_t = \max(\min(\lambda \beta_{t-1} \exp(s_t), 1 - \epsilon), \epsilon), \quad (21)$$

with  $\beta_1 = 0.5$  and learning rate  $\lambda > 0$ . The decision rule is:

$$\mathcal{D}_t^* = \begin{cases} \alpha_{\text{explore}}(\mathcal{D}_{\text{pool}}, b, \mathcal{M}_{t-1}), & \text{if } \beta_t \leq 0.5, \\ \alpha_{\text{exploit}}(\mathcal{D}_{\text{pool}}, b, \mathcal{M}_{t-1}), & \text{if } \beta_t > 0.5. \end{cases} \quad (22)$$

Thus,  $\beta_t$  dynamically adjusts the balance between exploration and exploitation based on the feedback metric, increasing the likelihood of exploitation when recent batches have yielded higher loss. The algorithm described above is written in Algorithm 2, featuring the integrated adaptive component. The choice of  $\beta_1 = 0.5$  is to ensure that the AL process starts with exploring the dataset rather than exploiting biased knowledge.

#### E. Annealing exploration structure

Another way to address the exploration-exploitation dilemma is to implement a selection mechanism with annealing behavior. This is inspired by the concept of cosine annealing learning rate in machine learning [40]. In this approach, exploration-oriented acquisition functions are applied exclusively during an initial phase of  $T_{\text{initial}}$  exploration AL iterations. After this, the process alternates between exploitation and exploration phases. The first exploitation phase lasts  $T_{\text{exploit}_1}$  iterations, followed by an exploration phase of fixed length  $T_{\text{explore}}$ . In subsequent cycles  $i \geq 1$ , the exploitation phase duration increases multiplicatively according to a rate  $r > 1$ , i.e.,  $T_{\text{exploit}_{i+1}} = \lfloor r \cdot T_{\text{exploit}_i} \rfloor$ . This results in gradually longer exploitation phases, while exploration phases remain constant in length, thus biasing the process toward exploitation as AL progresses. Formally, let  $\alpha_{\text{explore}}$  and

---

**Algorithm 2** Active learning with adaptive feedback structure using previous model loss on selected batches

---

Input: Neural network  $\mathcal{M} = f(x; \omega)$   
 Input: Unlabeled dataset  $\mathcal{D}_U$   
 Input: Initial number of samples  $M$ ,  
 Input: Total number of iterations  $T$   
 Input: Number of samples in a batch  $b$   
 Input: Acquisition functions with exploration  $\alpha_{\text{exploration}}$   
     and exploitation  $\alpha_{\text{exploitation}}$  paradigms  
 Input: Size of metric window  $n_{\text{window}}$  and the learning  
     rate of the feedback loop  $\lambda$   
 1: Initialize  $\beta_1 = 0.5$  and  $\epsilon = 0.1$ .  
 2: Initialize  $L$  an empty list of previous model loss on  
     the selected batch.  
 3: Labeled dataset  $\mathcal{D}_L \leftarrow M$  examples drawn randomly  
     from  $\mathcal{D}_U$  together with queried labels.  
 4: Train an initial model  $\mathcal{M}_0$  on  $\mathcal{D}_L$ .  
 5: for  $t = 1, \dots, T$  do  
 6:   ▷ Selecting acquisition function  
 7:   if  $\beta_t \leq 0.5$  then  
 8:     Use exploration acquisition function  
 $\alpha_{\text{exploration}}$ .  
 9:   else  
 10:    Use exploitation acquisition function  
 $\alpha_{\text{exploitation}}$ .  
 11:   end if  
 12:   ▷ Acquisition of batch  
 13:   Draw  $\mathcal{D}_{\text{pool}}$  randomly from  $\mathcal{D}_U$ .  
 14:   Select  $b$  sample  $\mathcal{D}_t^* = \alpha(\mathcal{D}_{\text{pool}}, b, \mathcal{M}_{t-1})$ .  
 15:    $\mathcal{D}_U \leftarrow \mathcal{D}_U \setminus \mathcal{D}_t^*$ .  
 16:    $\mathcal{D}_L \leftarrow \mathcal{D}_L \cup \mathcal{D}_t^*$ .  
 17:   Train a model  $\mathcal{M}_t$  on  $\mathcal{D}_L$  by getting  
 $\omega_t = \arg \min_{\omega} J(\mathcal{D}_L, \omega)$ .  
 18:   ▷ Computing trade-off parameter  
 19:   Add previous model loss on selected batch  
 $J(\mathcal{D}_t^*, \omega_{t-1})$  to  $L$ .  
 20:   Extract previous model loss subset  
 $L' = L[t - n_{\text{window}}; t]$ .  
 21:   Compute moving average on subset  $L' = MA(L')$ .  
 22:   Compute scaled score :  $s_t = \frac{L'[-1] - \min(L')}{\max(L') - \min(L')}$ .  
 23:   Compute trade-off score :  
 24:    $\beta_t = \max(\min(\lambda \beta_{t-1} \exp(s_t), 1 - \epsilon), \epsilon)$ .  
 25: end for  
 26: return Final model  $\mathcal{M}_T$ .

---

$\alpha_{\text{exploit}}$  denote the respective acquisition functions. At each iteration  $t$ , the selected batch is given by:

$$\mathcal{D}_t^* = \begin{cases} \alpha_{\text{explore}}(\mathcal{D}_{\text{pool}}, b, \mathcal{M}), & \text{if } t \text{ is in an exploration phase,} \\ \alpha_{\text{exploit}}(\mathcal{D}_{\text{pool}}, b, \mathcal{M}), & \text{if } t \text{ is in an exploitation phase.} \end{cases} \quad (23)$$

The schedule of exploration and exploitation phases is determined by  $T_{\text{initial exploration}}$ ,  $T_{\text{exploit}_1}$ ,  $T_{\text{explore}}$ , and  $r$ .

#### F. Random exploration structure

In this structure, we simply alternate between two acquisition functions randomly without any kind of feed-

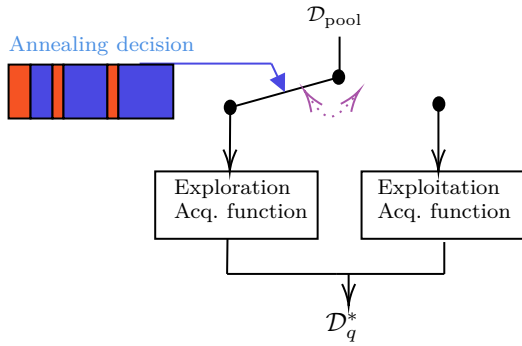


Fig. 4. Annealing exploration structure

back from the quality of the selected batch. Formally, let  $\{\alpha_1, \alpha_2\}$  be the two acquisition functions considered. At round  $t$ , draw  $I_t \sim \text{Uniform}\{1, 2\}$  and select  $\mathcal{D}_t^* = \alpha_{I_t}(\mathcal{D}_{\text{pool}}, b, \mathcal{M})$ , where  $\mathcal{M}$  is the current model and  $\mathcal{D}_{\text{pool}}$  is the unlabeled data pool. This approach serves as a baseline to evaluate whether more sophisticated alternation strategies offer measurable improvements.

## V. Experiments

### A. Experimental settings

#### 1) Dataset and models:

a) CIFAR: The CIFAR datasets [41] are widely used compilations of real-world images, facilitating comparisons in deep learning tasks for computer vision. Named after the Canadian Institute for Advanced Research, these datasets consist of color images representing various real-world objects. The CIFAR datasets have become a standard for establishing baselines in deep learning.

The CIFAR10 dataset contains 60,000 images, each sized at  $32 \times 32$  pixels and in color. These images are divided into 10 distinct categories, with 6000 images assigned to each category. It is split into a training set of 50,000 images and a test set of 10,000 images. The test set includes 1000 randomly selected images for each category. Similarly, the CIFAR100 dataset comprises 60,000 images, also  $32 \times 32$  pixels in size and in color, but grouped into 100 classes, each with 600 images. Within each class, there are 500 training images and 100 testing images. It is important to note that the CIFAR100 dataset presents more challenging scenarios compared to CIFAR10. This is primarily due to their increased number of class labels and reduced number of examples per class. For CIFAR datasets we consider the three following combinations of dataset and model:

- CIFAR10 and VGG16 which is VGG with 16 layers
- CIFAR10 and ResNet18 which is ResNet with 18 layers
- CIFAR100 and VGG16

b) PTB-XL: We extend our study to the ECG classification task, a time series classification problem essential for detecting cardiovascular diseases. The PTB-XL dataset [42] was selected due to its considerably larger sample size (over 18,000 individuals) compared to ECG5000 [43] (5,000 samples from a single patient). Our

experiments focus on the five coarse superclasses of PTB-XL. Following prior work [44], we adopt ResNet101, which has demonstrated strong performance on this dataset.

2) Implementation details: We implemented the ResNet, and VGG in Pytorch [45]. To implement the iterative workflow of AL we have used a version of modAL [46]. The implementation of the submodular-based acquisition functions utilizes the submodlib library [47]. More specifically the disparity min and FL acquisition functions work on the features of data obtained by computing the last hidden layer output from the model, this is known as the feature representation. For disparity min, the similarity metric used is cosine similarity  $\langle \vec{p}, \vec{q} \rangle = \frac{\vec{p} \cdot \vec{q}}{\|\vec{p}\| \|\vec{q}\|}$ , while for FL the distance used is also obtained via the cosine similarity  $d(\vec{p}, \vec{q}) = 1 - \text{similarity}(\vec{p}, \vec{q})$ .

The experiments were conducted on a laptop equipped with a Quadro RTX 5000 16 GB GPU (with driver version 545.23.08, and CUDA version 12.3), and a 10th Gen Intel(R) Core(TM) i9-10900K CPU operating at 3.70 GHz. The system was configured with 64.0 GB of RAM and ran on the Ubuntu operating system.

3) Hyperparameters: We performed ablations of the query batch size  $b$  and pool size  $|\mathcal{D}_{\text{pool}}|$  hyperparameters on CIFAR10. We determined that the optimal query batch size is 800 for CIFAR10 while for the pool size, we found out that  $|\mathcal{D}_{\text{pool}}| = 8000$  is a good balance. For CIFAR100, we chose  $b = 400$ ,  $|\mathcal{D}_{\text{pool}}| = 4000$ , a learning rate of 0.001, and we ran 30 acquisition rounds. For both datasets, we consider a learning rate of 0.001 and 40 epochs at each AL round. We run  $N_{\text{MC-Dropout}} = 5$  MC-Dropout iterations at the inference phase when required by the acquisition function.

4) Winning rate using  $t$ -test: Assessing the superiority of different acquisition functions poses multiple challenges. Firstly, due to the intricate nature of machine learning models and diverse datasets, one has to conduct several experimental setups in order to be sure that the AL strategy considered is better generally and not only on edge cases. Secondly, due to the inherent stochastic nature of training, it is necessary to repeat the training process several times. Moreover, the iterative nature of AL involves that the acquisition function can perform well in the first rounds and worse later. This is why we create a winning rate which can handle the above-mentioned difficulties. To accomplish this, we evaluate strategies using pairwise comparisons, a method extensively utilized in the AL literature [22], [18]. We repeat each experimental setup, with  $N$  different seeds, and obtain a set of  $N$  accuracy results  $a_r = \{a_{r,1}, \dots, a_{r,N}\}$  in each round  $r$ . A two-sided  $t$  test is performed. Let  $a_r^i$  and  $a_r^j$  be the set of accuracy scores for two different AL strategies  $i$  and  $j$  at AL round  $r$ . Then, the  $t$ -score is formulated as:

$$t_r^{ij} = \frac{\sqrt{N} \mu_r^{ij}}{\sigma_r^{ij}} \quad \text{where} \quad \mu_r^{ij} = \frac{1}{N} \sum_{l=1}^N (a_{r,l}^i - a_{r,l}^j),$$

$$\text{and} \quad \sigma_r^{ij} = \sqrt{\frac{1}{N-1} \sum_{l=1}^N ((a_{r,l}^i - a_{r,l}^j) - \mu_r^{ij})^2}. \quad (24)$$

K-Centers	0	14	14	19	24	19	29	29	14	18
BADGE	29	0	29	29	43	19	29	29	33	27
BALD	48	38	0	10	43	24	38	19	48	30
Entropy	52	43	33	0	38	38	52	43	62	40
Least confident	48	33	24	14	0	24	24	33	38	26
Margin sampling	52	38	24	14	38	0	38	48	29	31
Mean STD	43	52	29	19	29	24	0	33	29	29
PowerBALD	19	38	29	19	38	29	48	0	33	28
Random sampling	33	29	33	14	29	14	24	33	0	23
K-Centers		BADGE	BALD	Entropy	Least confident	Margin sampling	Mean STD	PowerBALD	Random sampling	

Fig. 5. Heatmap illustrating the pairwise comparison of winning rates on CIFAR10 VGG of baseline acquisition functions. The last column represents the row average (the higher the better).

Here, the strategy  $i$  is considered to beat the strategy  $j$  if  $t_r^{ij} > 2.776$  with 2.776 being the critical point of  $p$ -value being 0.05. Therefore, given  $R$  acquisition rounds, one can define the winning rate formulated as follows:

$$\text{win}^{ij} = \sum_{r=1}^R \frac{1}{R} \mathbf{1}_{t_r^{ij} > 2.776} \quad (25)$$

The value of the winning rate becomes 1 if the strategy  $i$  beats the strategy  $j$  over all AL rounds.

5) Pairwise comparison using heatmaps: In order to compare each acquisition function on each set of experiments, we plot the heatmaps (like Fig. 5) using the winning rate as introduced ahead. Therefore, one can easily compare acquisition functions. The last column on the right of the heatmap represents the mean of each row, which means that it represents on average how much the considered acquisition function wins over the others: the higher the better.

## B. Baseline

In order to set a baseline, we evaluate the following acquisition functions: BADGE, BALD, entropy,  $K$ -Centers, least confident, margin sampling, mean STD, PowerBALD, and random sampling (selecting samples randomly, like passive learning). BAIT acquisition function was not included in the baseline due to its higher computational cost and lack of accuracy gains, as our focus is on sustainable acquisition functions.

In order to highlight the relative performance, the baseline acquisition functions are compared on CIFAR10 with VGG, with the winning rates reported in Fig. 5. One can observe that  $K$ -Center is the worst acquisition function with an average winning rate of 18%. Meanwhile, BADGE performs well enough in comparison to other acquisition functions with an average winning rate of 26%. The acquisition functions based explicitly on uncertainty paradigms are hard to beat with other approaches like  $K$ -Centers or BADGE.

In Table I, the comparison between the average winning rate of the baselines reveals that there is no huge rank

TABLE I

Comparison of average winning rate (AWR) of baseline acquisition functions against themselves on the considered datasets with their associated rank (R).

	CIFAR10 VGG		CIFAR10 ResNet		CIFAR100 VGG		PTB-XL ResNet101	
Acq. Func.	AWR	R	AWR	R	AWR	R	AWR	R
BADGE	27	6	36	3	24	7	48	1
BALD	30	3	43	2	47	1	40	2
Entropy	40	1	30	5	11	9	39	3
<i>K</i> -Centers	18	9	9.6	9	39	2	5	9
Least confident	26	7	33	4	29	6	35	4
Margin sampling	31	2	28	6	31	4	21	7
Mean STD	29	4	52	1	30	5	29	6
PowerBALD	28	5	20	8	37	3	19	8
Random sampling	23	8	23	7	20	8	30	5

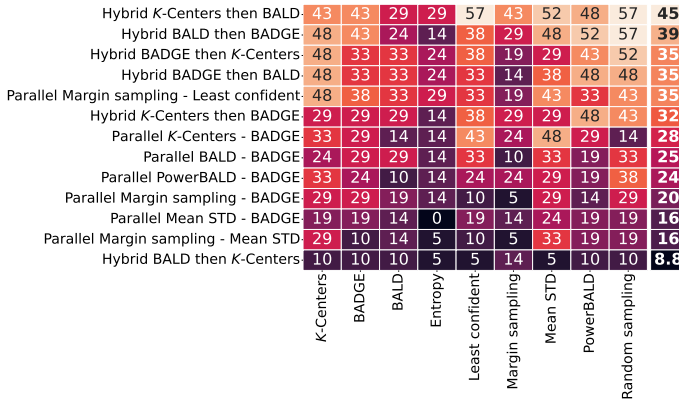


Fig. 6. Heatmap illustrating pairwise comparison of winning rates on CIFAR10 VGG of multiple Parallel and Hybrid combinations of acquisition functions against baseline acquisition functions.

change between the results of CIFAR10 and CIFAR100, except for *K*-Centers and entropy, when using the same model. By comparing the results on CIFAR10 using ResNet with the one using VGG, it is evident that there is a huge change in rank and average winning rate between ResNet and VGG results on CIFAR10. The PTB-XL dataset, consisting of time series data, clearly shows the ineffectiveness of *K*-Centers, while BADGE proves highly effective, reaching a 48% average winning rate. This result highlights the ranking variations caused by domain differences with respect to image datasets. *K*-Centers relies on the assumption that feature-space distance results in informational diversity. That assumption holds better for structured visual datasets like CIFAR-10 than for noisy, high-variability biomedical signals like PTB-XL, where embeddings in early AL stages are not yet reliable for diversity-based selection.

### C. Results of Parallel and Hybrid structures

For the parallel-ranked combinations, we assessed various pairs of acquisition functions on CIFAR-10 with VGG, including BALD, Margin Sampling, PowerBALD, Least Confident, and Mean STD. None of these pairs demonstrated any improvement, achieving only a 10% average winning rate against the baseline. In fact, they significantly reduced performance compared to the original performance of each individual component in the pairs.

In the Parallel structure, we evaluated several pairs of acquisition functions on CIFAR-10 using the VGG model: BADGE and BALD, BADGE and *K*-Centers, BADGE and mean STD, BADGE and PowerBALD, BADGE and margin sampling, margin sampling and mean STD, and margin sampling and least confident. As shown in Figure 6, the average winning rate of parallel combinations of acquisition functions against the baseline does not exceed 28%. Among these combinations, Parallel *K*-Centers - BADGE achieved the highest average performance. However, splitting the pool into two parts often leads to selecting highly similar samples, exacerbating batch selection issues. The performance of Parallel structures does not justify the additional computational expense of running two acquisition functions.

### D. Results of Series structure

Here we consider the combination of two acquisition functions with the first acquisition function selecting  $\kappa b = 2b$  samples on which the second acquisition function selects  $b$  samples, where  $b$  is the budget for one round of AL. An ablation of the  $\kappa$  could be run to see if larger or smaller  $\kappa$  would result in performance improvement with a time trade-off. The series structure allows us to aggregate two acquisition functions based on two different criteria. We consider 16 different aggregations of uncertainty-based acquisition functions, namely BALD and BADGE, with representativity-based or diversity-based ones such as FL, disparity min, feature-based, *K*-Centers, or BADGE.

As expected, the aggregated acquisition functions perform generally well when first running an uncertainty based function to reduce the choice of samples and then running a diversity or representativity-based function. This is shown in Fig. 7 for CIFAR10 VGG. The best score belongs to Series BALD then Disparity min with an average winning rate of 52%. This is due to the fact that BALD selects highly similar samples and uses disparity min hence allowing us to ensure diversity among the samples that are the most informative according to BALD.

The fact that both Series BADGE then FL and Series BALD then FL achieve a winning rate of at least 43% against BALD and BADGE demonstrates the effectiveness of incorporating a representativity step. The most surprising finding is that using FL after BADGE outperforms using BADGE alone, even though BADGE already includes a clustering step. This improvement may be attributed to FL leveraging the model's knowledge via the feature representation in the last hidden layer, rather than relying solely on the uncertainty derived from MC-Dropout. Interestingly, Series BADGE then *K*-Centers does not yield significant improvements, achieving a winning rate of only 29% against BALD and BADGE..

Surprisingly, combining representativity-based acquisition functions with uncertainty-based ones also performs well. For instance, Series *K*-Centers then BALD achieves an average winning rate of 50%. Similarly, aggregated functions like Series BALD then Disparity min and Series

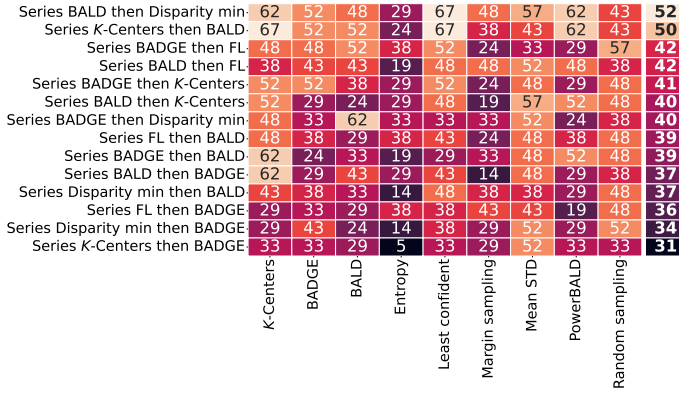


Fig. 7. Heatmap illustrating pairwise comparison of winning rates on CIFAR10 VGG of multiple series combinations of uncertainty and representativity or diversity based acquisition functions against baseline acquisition functions.

*K*-Centers then BALD show a strong winning rate of 52% against both BALD and BADGE. This finding is interesting as it suggests the potential to sample a larger pool and then apply algorithms to select the most representative samples.

We ran Series *K*-Centers then BALD and Series BALD then Disparity min which are the best Series acquisition functions on CIFAR10 using ResNet, on CIFAR100 using VGG, and on PTB-XL using ResNet101. The results are presented in Fig. 10, Fig. 11 and Fig. 12. The good result of the Series structure can also be observed on CIFAR100 using VGG: Series *K*-Centers then BALD has an average winning rate of 53% against the baseline, while Series BALD then Disparity min has an average winning rate of 36% but with good performance against Entropy, BADGE or *K*-Centers. For CIFAR10 using ResNet, the results are less promising with around 30% of average winning rate. On the ECG classification task, which is a completely different domain from image classification, Series BALD then Disparity min performs well, as shown in Fig. 12, with an average winning rate of 52%. However, this is not the case for Series *K*-Centers then BALD, which particularly underperforms with an average winning rate of 9%. The reason is that *K*-Centers alone performs particularly poorly on the PTB-XL dataset with an average winning rate of 5%, thereby harming the performance of the combined strategy.

To evaluate how the  $\kappa$  parameter affects the performance of the series structure, experiments were conducted using the Series *K*-Centers then BALD approach. Twenty experiments were run for each  $\kappa$  value on CIFAR-10 using VGG, with a subpool of 8,000 samples, a query batch size of 200, and 40 acquisition iterations. BALD and *K*-Centers were run as baselines for comparison. The experimental design ensures that  $\kappa = 1$  corresponds to running *K*-Centers alone, while  $\kappa = 40$  corresponds to running BALD alone. The results in Fig. 8 clearly confirm our earlier findings: *K*-Centers is faster than BALD, but BALD achieves better accuracy. Consequently, Series *K*-Centers then BALD yields better accuracy than BALD alone. The key insight from this experiment is that Series *K*-

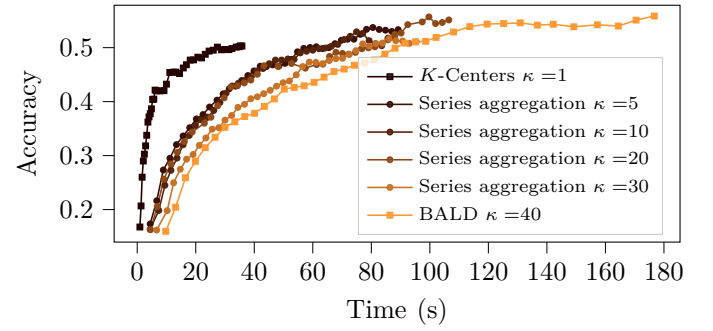


Fig. 8. Accuracy over time for Series *K*-Centers then BALD with different ratio  $\kappa$  values on CIFAR10 VGG. *K*-Centers and BALD results are represented as baseline.

Centers then BALD performs better with respect to both objectives (time and accuracy) with minimal sensitivity to the  $\kappa$  parameter. As shown in Fig. 8, the time required to achieve the same accuracy as BALD is reduced by half in this example when choosing  $\kappa = 20$ . It gives almost the same result as  $\kappa = 5$ . Mostly the sub-pool size of selected by *K*-Centers has to be large enough in order for BALD to select relevant points, but large enough so that it reduces the overall computational time.

The computational efficiency gain can be quantified by analyzing the number of model inferences required, as inference constitutes the most computationally expensive component of acquisition function evaluation. Let  $N_{\text{infer}}$  denote the total number of model inferences required by an acquisition function. For BALD,  $N_{\text{infer}} = N_{\text{MC-Dropout}} \cdot |\mathcal{D}_{\text{pool}}|$ , while for *K*-Centers,  $N_{\text{infer}} = |\mathcal{D}_{\text{pool}}| + |\mathcal{D}_{\mathcal{L}}|$ . For the proposed Series *K*-Centers then BALD approach, the total inference count is  $N_{\text{infer}} = |\mathcal{D}_{\text{pool}}| + |\mathcal{D}_{\mathcal{L}}| + \kappa b N_{\text{MC-Dropout}}$ , where  $\kappa b \ll |\mathcal{D}_{\text{pool}}|$ . Beyond the computational speedup, *K*-Centers is specifically designed to exploit sample representativity, thereby promoting sample diversity. This enhanced diversity may account for the observed accuracy improvements relative to BALD alone.

## E. Results of Hybrid structure

In order to evaluate the effectiveness of the hybrid structure, we combine BALD, BADGE, and *K*-Centers with each other, resulting in 6 acquisition functions to discuss. From the first glance at Fig. 6, one can observe that the hybrid combinations are better than the parallel ones with higher winning rates against the baselines. However, it is apparent that this type of structure does not compare favorably to the series structure. For instance, Hybrid BADGE then *K*-Centers achieves an average winning rate of 35% against the baseline, whereas Series BADGE then *K*-Centers achieves 40%. Moreover, the Hybrid structure incurs higher costs than the Series structure. In the Series structure, the second acquisition function operates on samples selected within the batch by the first acquisition function, whereas in the Hybrid structure, the second function operates on the entire pool excluding the previously selected samples, which is

more costly. Although the Hybrid structure mitigates the disadvantage of the Parallel structure, which splits the pool into two parts resulting in the selection of highly similar samples, the results do not exceed those of series combinations. Consequently, the Hybrid structure does not justify its cost compared to the Series combination.

#### F. Results of Adaptive feedback structure and of structures switching between acquisition functions

To evaluate the combination of acquisition functions, we selected three uncertainty-based functions: BALD, entropy, and least confident. These were combined with two diversity-based functions: BADGE and disparity min, as well as two representativeness-based functions:  $K$ -Centers and FL. For each dataset, we evaluate the performance of the following acquisition functions: random sampling, BALD, PowerBALD,  $K$  Centers, BADGE, mean STD, max entropy, least confident. We benchmark combinations using adaptive feedback with loss of the previous model on the selected batch, random and annealing structures. Please note that for the annealing structure, we have chosen  $T_{\text{initial exploration}} = 5$ ,  $r = 1.5$ ,  $T_{\text{exploit}_1} = 5$ ,  $T_{\text{explore}} = 5$ , as we run VGG on CIFAR10 for 20 rounds only here, this choice makes it such that exploration strategy is chosen for the 5 first rounds, then exploitation for the 5 next, then exploration for the 5 next, and finally exploitation for the 5 next. On CIFAR10 with VGG, we evaluated the combinations against the baseline in Fig. 9. In Fig. 9, it is evident that the three top combinations are Random Least confident - FL, Annealing BALD - BADGE and Annealing Least Confident - BADGE. These three combinations outperform on average with more than 54% winning rate over the baseline.

Here we considered BADGE as the exploration function (as it is based on the diversity of gradients) and BALD as the exploitation function (as it is an uncertainty-based method). However, the acquisition functions Random BALD - BADGE and in particular Annealing BALD - BADGE works better than Adaptive feedback BALD - BADGE with 50% average winning rate on CIFAR10 for VGG. This suggests that simply alternating between BADGE and BALD with annealing or random structure could be more important than alternating between BADGE and BALD at the right moment with adaptive feedback.

This result remains surprising, considering that both BADGE and BALD aim to maximize the same objective — expected information gain, as outlined in [48]. The main distinction lies in BADGE's design, which addresses BMAL pathologies by emphasizing sample representativeness through  $k$ -Means++ clustering on gradient embeddings, categorizing it as a diversity-based acquisition function. This emphasis on clustering might explain why combinations of BADGE and BALD achieve a winning rate of more than 50% over BALD, which operates in a Top- $K$  manner. However, it does not fully elucidate why it outperforms BADGE alone. One plausible interpretation is rooted in the differing operational spaces:

BALD operates in prediction space (via MC-Dropout), while BADGE operates in weight space (via gradient embedding). Alternating between these spaces may synergistically enhance the final acquisition function's efficacy. This approach effectively addresses the problem from two distinct perspectives, potentially leading to improved overall performance.

To observe if the results are stable while changing the dataset and model, we run Adaptive Feedback BALD - BADGE, Annealing BALD - BADGE, Random BALD - BADGE, Adaptive Feedback Least confident - FL, Annealing Least confident - FL, and Random Least confident - FL on CIFAR10 using ResNet on CIFAR100 using VGG, and on PTB-XL using ResNet101. The results are presented in Fig. 10, in Fig. 11, and in Fig. 12. The good result of the alternating structure can also be observed on CIFAR10 using ResNet: with Adaptive Feedback BALD - BADGE and Annealing BALD - BADGE achieving 56% and 49% of average winning rate respectively. For CIFAR100 using VGG, the results are less promising with the best alternating acquisition function achieving an average winning rate of 37% but with good performance against Entropy, and BADGE. Although ECG classification represents a completely different domain from image classification, Fig. 12 shows that Adaptive Feedback BALD - BADGE and Annealing BALD - BADGE are again the top acquisition functions, each attaining an average winning rate of 58%.

To investigate the influence of the period rate  $r$  on the Annealing structure, five values of  $r$  ranging from 1 to 2 were evaluated. For each value, twenty experiments were conducted on CIFAR-10 using VGG, with a subpool size of 5,000 samples, a query batch size of 500, and 40 acquisition iterations. The results are shown in Fig. 13. The settings  $r = 1$  and  $r = 1.2$  yielded the highest performance, although the results for  $r = 2$  were comparable in terms of both accuracy and runtime. Notably,  $r = 1$  corresponds here to the case where the exploration and exploitation acquisition functions operates equally, the result should be similar to Random BALD - BADGE. However, starting with BADGE for a predefined number of iterations  $T_{\text{initial exploration}}$ , and restarting for  $T_{\text{exploration}}$  iterations after  $T_{\text{exploitation}}$  iterations appears to produce significant improvements.

#### G. Robustness and energy gain of aggregated acquisition functions

In order to assess the execution duration for reaching a particular value of accuracy, we run the same experiment (CIFAR10 and VGG, 40 epochs of training at each round, a query batch size of 800, a pool size of 8000) until the model reaches 80% of accuracy or until the AL process excess one hour of execution time. The averaged results of 12 repetitions of experiments are compiled in Table II. It reveals that in terms of execution duration,  $K$ -Centers finishes on average the first with 28 minutes the first when it is able to reach 80% within one hour. However,  $K$ -Centers finishes before one hour only 2 times over

TABLE II

Comparison of acquisition functions when first having reached 80% of accuracy for CIFAR10 using VGG averaged in 12 repetitions of AL process (AL processes are stopped after reaching 80% of accuracy or after one hour of execution)

Acquisition function used	Execution duration	Acq. round	# samples	% of dataset	Final accuracy	# goal reached
Entropy	38min 7s	30	24000	40%	80%	3 out of 12
BALD	55min 26s	35	28000	46%	81%	2 out of 12
Least confident	35min 5s	28	22666	37%	82%	3 out of 12
PowerBALD	35min 58s	27	22133	36%	80%	3 out of 12
<i>K</i> -Centers	28min 21s	26	20800	34%	80%	2 out of 12
BADGE	47min 12s	31	24960	41%	81%	5 out of 12
Margin sampling	38min 44s	29	23800	39%	81%	4 out of 12
Series <i>K</i> -Centers then BALD	34min 21s	26	21333	35%	80%	6 out of 12
Adaptive feedback BALD - BADGE	39min 12s	31	25066	41%	80%	3 out of 12
Random BALD - BADGE	40min 51s	29	23866	39%	80%	6 out of 12
Annealing BALD - BADGE	45min 34s	32	25733	42%	80%	6 out of 12

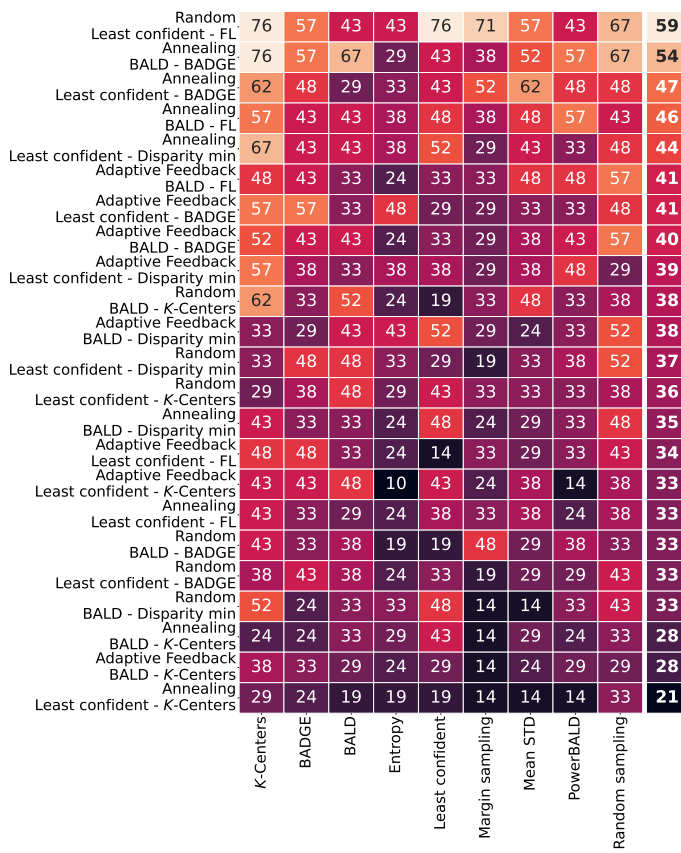


Fig. 9. Heatmap illustrating pairwise comparison of winning rates on CIFAR10 VGG of multiple Adaptive feedback combinations against baseline acquisition functions.

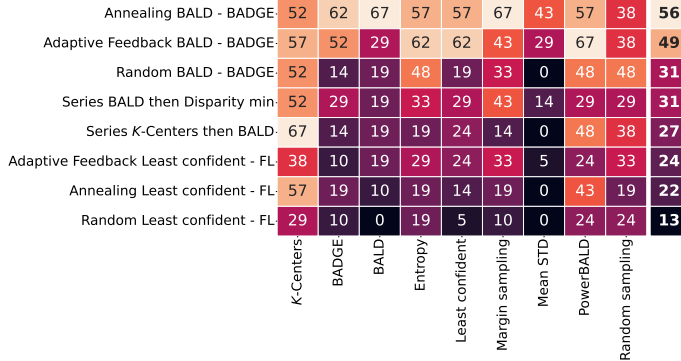


Fig. 10. Heatmap illustrating pairwise comparison of winning rates on CIFAR10 using ResNet of multiple combinations of acquisition function against baseline acquisition functions.

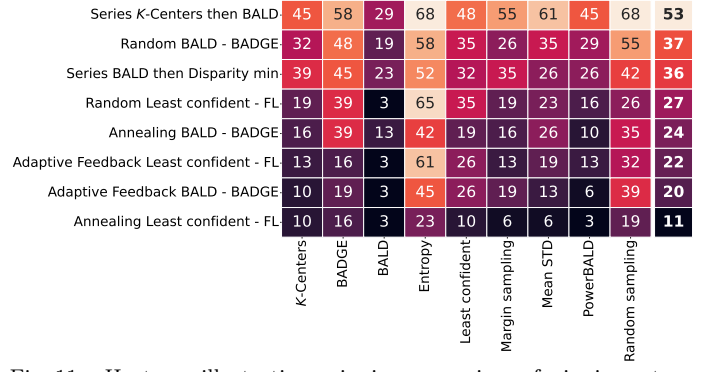


Fig. 11. Heatmap illustrating pairwise comparison of winning rates on CIFAR100 using VGG of multiple combinations of acquisition function against baseline acquisition functions.

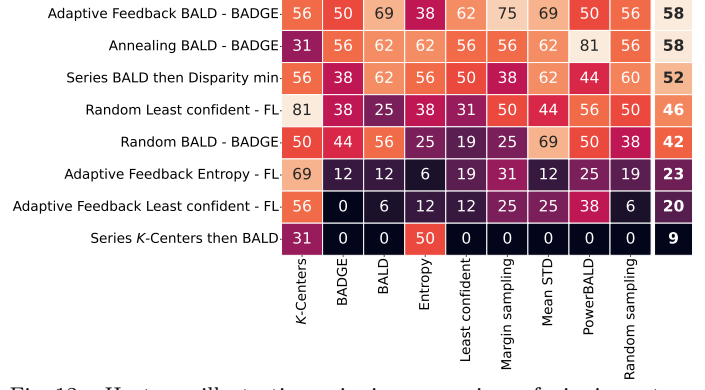


Fig. 12. Heatmap illustrating pairwise comparison of winning rates on PTB-XL using ResNet101 of multiple combinations of acquisition function against baseline acquisition functions.

12 repetitions of AL process. Executing BALD on the subpool extracted using *K*-Centers brings this number from 2 successes to 6 successes over 12 repetitions. When Series *K*-Centers then BALD succeeds reaching 80% of accuracy, able to do it in 9 acquisition rounds less than with BALD alone. In terms of labeling cost, this represents  $9 \times 800 = 7200$  labels less, as a query batch size of  $b = 800$  was used. Regarding the entirety of CIFAR10, this represents 12% of the total available samples. This means that for the same accuracy goal, one needs 12% of energy less to train the model. Actually, the cost of energy for training a model depends directly on the number of samples selected.

The methods combining BALD and BADGE are also

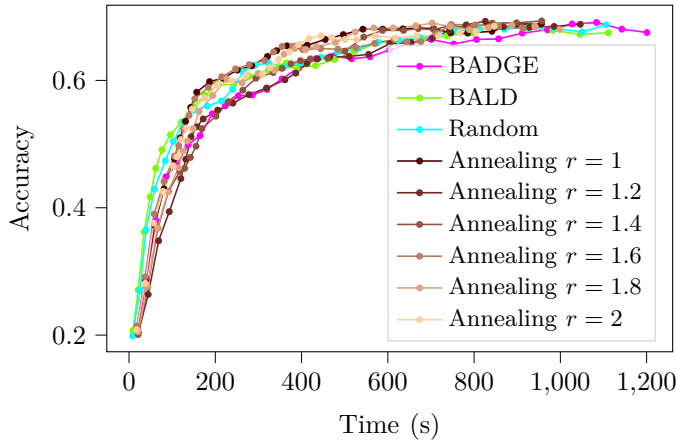


Fig. 13. Accuracy over time for Annealing BALD BADGE with different annealing rate  $r$  values on CIFAR10 VGG. Random BALD BADGE, BALD and BADGE results are represented as baseline.

more robust in terms of reaching 80% accuracy before one hour, achieving success 6 times over 10 for Random BALD - BADGE and Annealing BALD - BADGE. They are also better in terms of execution time than BALD and BADGE alone. Regarding the energy cost, the same argument can be developed for the aggregated functions Random BALD - BADGE and Annealing BALD - BADGE. However, our experiment did not reveal the same improvement range in number of rounds to reach the same objective as from using Series  $K$ -Centers then BALD instead of  $K$ -Centers or BALD alone, but it still improves the robustness of the acquisition functions.

On top of this data-efficiency gain, we already discussed the potential gain in terms of the execution duration of the series and adaptive feedback structure. In fact, we have shown that the series structure if the acquisition functions are well chosen can lead to a reduction in execution time compared to one alone without loss of accuracy. This is the case for Series  $K$ -Centers then BALD which requires fewer acquisition rounds. The difference arises from the fact that BALD requires  $N_{MC\ dropout}|\mathcal{D}_{pool}|$  forward passes, whereas  $K$ -Centers requires only  $|\mathcal{D}_{pool}|$  forward passes. Applying BALD on top of  $K$ -Centers requires only  $|\mathcal{D}_{pool}| + N_{MC\ dropout}b << N_{MC\ dropout}|\mathcal{D}_{pool}|$  forward passes. Moreover, concerning adaptive feedback structure, there is at least no escalation of the running time of the acquisition functions itself. Our proposed structures, therefore, at least, do not lengthen the execution time of acquisition functions, and in certain scenarios, even shorten it. Considering that energy consumption is proportional to the execution time, our proposed structures also do not escalate the energy costs of active learning processes, and in some cases, they even reduce it. We experimentally demonstrated that our proposed structures can achieve data-efficiency gain without increasing the overhead computation cost of AL.

By wisely selecting the structures and the acquisition functions, we are able to obtain gain in terms of both

the quality of the data selected and the efficiency of the method to select them, leading to an overall energy gain.

## H. Key practical insights

Based on the comprehensive experimental results presented in this work across various datasets and model architectures, several key factors emerge as critical determinants of AL performance and the effectiveness of aggregated acquisition functions in terms of accuracy:

- Model architecture interactions play a crucial role, as evidenced by the substantial changes in ranking between VGG and ResNet results on CIFAR-10, as discussed in Section V-B.
- Batch mode pathologies significantly affect performance: Top- $K$  selection tends to amplify redundancy issues in parallel-ranked structures (see Section V-C), whereas series structures mitigate these problems through progressive filtering (see Section V-D).
- Alternating strategies, such as switching between multiple methods, yet simple prove to be essential: approaches alternating between BADGE and BALD consistently achieve winning rates above 50% across domains, as they operate in complementary spaces (weight vs. prediction). This is observed for Random BALD-BADGE, Annealing BALD-BADGE, and Adaptive Feedback BALD-BADGE (see Section V-F). In a similar vein, the results of Hybrid BADGE then BALD presented in Section V-C can also be interpreted as stemming from this complementary behavior.
- Domain appears to be a key determinant for some acquisition functions: the feature space assumptions underlying diversity-based methods like  $K$ -Centers may not translate effectively to time series data, where early-stage embeddings are often unreliable, as shown in Section V-B. Therefore the superior performance of Series  $K$ -Centers then BALD on structured visual datasets such as CIFAR-10/100 (achieving winning rates above 50%) contrasts sharply with its poor performance on the noisy, high-variability PTB-XL ECG dataset (9% winning rate) as denoted in Section V-D.

These findings indicate that successful aggregation depends on careful consideration of dataset characteristics, architectural compatibility, and the underlying principles of the constituent acquisition functions, rather than on a one-size-fits-all combination strategy. While most findings were validated across CIFAR10, CIFAR100, and PTB-XL, the relative strength of each aggregation structure varied. This reinforces the need to test acquisition functions in the target domain rather than relying on benchmarks alone.

To improve performance in terms of computation time while keeping the number of acquisition iterations constant, only the series structure was able to reduce computational time by progressively decreasing the pool size (see Section V-D).

## VI. Conclusion and Future Works

Active learning is a powerful technique that can reduce the number of samples necessary for model training to achieve a specified accuracy. This reduction not only lowers labeling costs but also leads to energy savings during the training of neural network models. Therefore, it is a learning method that can promote both data efficiency and energy efficiency. In this paper, we implemented and compared various state-of-the-art acquisition functions in terms of accuracy and computational costs. To address the exploration-exploitation dilemma, we introduced six types of aggregation structures: series, parallel, hybrid, adaptive feedback, random exploration, and annealing exploration. After conducting ablation studies on hyperparameters, we compared the aggregated acquisition functions to a set of state-of-the-art baseline acquisition functions in terms of both energy cost and accuracy.

In these comparisons, two predominant structural types emerged. The series structure, in particular, showed a reduction in computational cost by using one acquisition function to initially reduce the pool size before applying the second one. Notably, combinations such as  $K$ -Centers followed by BALD demonstrated superior performance compared to BALD alone in two dataset-model pairs. This approach reduced the acquisition cost by almost half and decreased the number of labels needed to reach 80% accuracy by 12%. On the other hand, structures that alternate between exploration-based and exploitation-based acquisition functions at each round—whether based on a metric (adaptive feedback), the round number (annealing), or randomly (random)—have shown robust results.

In future work, we aim to address the query batch size parameter,  $b$ . Implementing a flexible query batch size could lead to further improvements in energy efficiency. This might involve adjusting the query batch size through an annealing process, initially exploring more to refine the model and accurately capture boundary decisions using acquisition functions. Another approach could involve treating  $b$  as a penalty term in an optimization process or using the information score of submodular functions to measure the benefit of adding a sample, ultimately excluding it if it is not valuable enough.

## References

- [1] P. Ren, Y. Xiao, X. Chang, P.-Y. Huang, Z. Li, B. B. Gupta, X. Chen, and X. Wang, “A survey of deep active learning,” ACM computing surveys (CSUR), vol. 54, no. 9, pp. 1–40, 2021.
- [2] E. Strubell, A. Ganesh, and A. McCallum, “Energy and policy considerations for deep learning in nlp,” arXiv preprint arXiv:1906.02243, 2019.
- [3] D. Amodei and D. Hernandez. AI and compute. Accessed 03-08-2023. [Online]. Available: <https://openai.com/blog/ai-and-compute/>
- [4] R. Schwartz, J. Dodge, N. A. Smith, and O. Etzioni, “Green ai,” Communications of the ACM, vol. 63, no. 12, pp. 54–63, 2020.
- [5] D. R.-J. G.-J. Rydning, J. Reinsel, and J. Gantz, “The digitization of the world from edge to core,” Framingham: International Data Corporation, vol. 16, pp. 1–28, 2018.
- [6] S. Salehi and A. Schmeink, “Data-centric green artificial intelligence: A survey,” IEEE Transactions on Artificial Intelligence, 2023.
- [7] ———, “Is active learning green? an empirical study,” in 2023 IEEE International Conference on Big Data (BigData). IEEE, 2023, pp. 3823–3829.
- [8] J. Xu, W. Zhou, Z. Fu, H. Zhou, and L. Li, “A survey on green deep learning,” arXiv preprint arXiv:2111.05193, 2021.
- [9] C. Yin, B. Qian, S. Cao, X. Li, J. Wei, Q. Zheng, and I. Davidson, “Deep similarity-based batch mode active learning with exploration-exploitation,” in 2017 IEEE International Conference on Data Mining (ICDM), 2017, pp. 575–584.
- [10] G. R. Upala Junaida Islam, Kamran Paynabar and A. S. Iquebal, “Dynamic exploration-exploitation trade-off in active learning regression with bayesian hierarchical modeling,” IIE Transactions, vol. 0, no. 0, pp. 1–15, 2024. [Online]. Available: <https://doi.org/10.1080/24725854.2024.2332910>
- [11] C. Jung, S. Salehi, and A. Schmeink, “Active learning with alternating acquisition functions: Balancing the exploration-exploitation dilemma,” in 2024 IEEE International Conference on Big Data (BigData). IEEE, 2024, pp. 5755–5764.
- [12] B. Settles, Active Learning Literature Survey. University of Wisconsin-Madison Department of Computer Sciences, 2009.
- [13] Y. Gal, R. Islam, and Z. Ghahramani, “Deep bayesian active learning with image data,” Mar. 2017. [Online]. Available: <http://arxiv.org/abs/1703.02910>
- [14] N. Houlsby, F. Huszár, Z. Ghahramani, and M. Lengyel, “Bayesian active learning for classification and preference learning,” Dec. 2011. [Online]. Available: <http://arxiv.org/abs/1112.5745>
- [15] J. Zhu, H. Wang, T. Yao, and B. K. Tsou, “Active learning with sampling by uncertainty and density for word sense disambiguation and text classification,” in Proceedings of the 22nd International Conference on Computational Linguistics (Coling 2008), D. Scott and H. Uszkoreit, Eds. Manchester, UK: Coling 2008 Organizing Committee, Aug. 2008, pp. 1137–1144. [Online]. Available: <https://aclanthology.org/C08-1143>
- [16] C. E. Shannon, “A mathematical theory of communication,” 1948.
- [17] M. Kampffmeyer, A.-B. Salberg, and R. Jenssen, “Semantic segmentation of small objects and modeling of uncertainty in urban remote sensing images using deep convolutional neural networks,” in 2016 IEEE Conference on Computer Vision and Pattern Recognition Workshops (CVPRW), 2016, pp. 680–688.
- [18] A. Kirsch, S. Farquhar, P. Atighehchian, A. Jesson, F. Branchaud-Charron, and Y. Gal, “Stochastic batch acquisition: A simple baseline for deep active learning,” Sep. 2023. [Online]. Available: <http://arxiv.org/abs/2106.12059>
- [19] O. Sener and S. Savarese, “Active learning for convolutional neural networks: A core-set approach,” Jun. 2018. [Online]. Available: <http://arxiv.org/abs/1708.00489>
- [20] J. T. Ash, C. Zhang, A. Krishnamurthy, J. Langford, and A. Agarwal, “Deep batch active learning by diverse, uncertain gradient lower bounds,” Feb. 2020. [Online]. Available: <http://arxiv.org/abs/1906.03671>
- [21] D. Arthur and S. Vassilvitskii, “k-means++: the advantages of careful seeding,” in Proceedings of the eighteenth annual ACM-SIAM symposium on Discrete algorithms, ser. SODA ’07. USA: Society for Industrial and Applied Mathematics, Jan. 2007, pp. 1027–1035.
- [22] J. T. Ash, S. Goel, A. Krishnamurthy, and S. Kakade, “Gone fishing: Neural active learning with fisher embeddings,” Dec. 2021. [Online]. Available: <http://arxiv.org/abs/2106.09675>
- [23] S. Fujishige, Submodular functions and optimization. Elsevier, 2005.
- [24] G. L. Nemhauser, L. A. Wolsey, and M. L. Fisher, “An analysis of approximations for maximizing submodular set functions—i,” Mathematical Programming, vol. 14, no. 1, pp. 265–294, Dec. 1978. [Online]. Available: <https://doi.org/10.1007/BF01588971>
- [25] K. Wei, R. Iyer, and J. Bilmes, “Submodularity in data subset selection and active learning,” in Proceedings of the 32nd International Conference on Machine Learning. PMLR, Jun. 2015, pp. 1954–1963, ISSN: 1938-7228. [Online]. Available: <https://proceedings.mlr.press/v37/wei15.html>
- [26] P. B. Mirchandani and R. L. Francis, Discrete location theory, 1990.
- [27] A. Dasgupta, R. Kumar, and S. Ravi, “Summarization through submodularity and dispersion,” in Proceedings of the 51st Annual Meeting of the Association for Computational Linguistics (Volume 1: Long Papers), vol. 1, 2013, pp. 1014–1022.

[28] A. Englhardt, H. Trittenbach, D. Vetter, and K. Böhm, "Finding the sweet spot: Batch selection for one-class active learning," Philadelphia, PA: Society for Industrial and Applied Mathematics, Jan. 2020. [Online]. Available: <https://doi.org/10.1137/1.9781611976236>

[29] B. Settles and M. Craven, "An analysis of active learning strategies for sequence labeling tasks," in Proceedings of the 2008 Conference on Empirical Methods in Natural Language Processing, M. Lapata and H. T. Ng, Eds. Honolulu, Hawaii: Association for Computational Linguistics, Oct. 2008, pp. 1070–1079. [Online]. Available: <https://aclanthology.org/D08-1112>

[30] B. Demir, C. Persello, and L. Bruzzone, "Batch-mode active-learning methods for the interactive classification of remote sensing images," *IEEE Transactions on Geoscience and Remote Sensing*, vol. 49, no. 3, pp. 1014–1031, 2011.

[31] H. T. Nguyen and A. Smeulders, "Active learning using pre-clustering," in Proceedings of the Twenty-First International Conference on Machine Learning, ser. ICML '04. New York, NY, USA: Association for Computing Machinery, 2004, p. 79. [Online]. Available: <https://doi.org/10.1145/1015330.1015349>

[32] Y. Gu, Z. Jin, and S. C. Chiu, "Active learning combining uncertainty and diversity for multi-class image classification," *IET Computer Vision*, vol. 9, no. 3, pp. 400–407, 2015. [Online]. Available: <https://ietresearch.onlinelibrary.wiley.com/doi/abs/10.1049/iet-cvi.2014.0140>

[33] S. Ebert, M. Fritz, and B. Schiele, "Ralf: A reinforced active learning formulation for object class recognition," in 2012 IEEE Conference on Computer Vision and Pattern Recognition, 2012, pp. 3626–3633.

[34] Y. Cheng, Z. Chen, L. Liu, J. Wang, A. Agrawal, and A. Choudhary, "Feedback-driven multiclass active learning for data streams," in Proceedings of the 22nd ACM international conference on Conference on information & knowledge management - CIKM '13. San Francisco, California, USA: ACM Press, 2013, pp. 1311–1320. [Online]. Available: <https://doi.org/10.1145/2505515.2505528>

[35] A. Tran, C. S. Ong, and C. Wolf, "Combining active learning suggestions," vol. 4, p. e157. [Online]. Available: <https://peerj.com/articles/cs-157>

[36] Y. Baram, R. El-Yaniv, and K. Luz, "Online choice of active learning algorithms," in Proceedings of the Twentieth International Conference on International Conference on Machine Learning, ser. ICML'03. AAAI Press, 2003, p. 19–26.

[37] R. Hu, S. Jane Delany, and B. Mac Namee, "Egal: Exploration guided active learning for tcb," in Case-Based Reasoning, Research and Development, I. Bichindaritz and S. Montani, Eds. Berlin, Heidelberg: Springer Berlin Heidelberg, 2010, pp. 156–170.

[38] S. Flesca, D. Mandaglio, F. Scala, and A. Tagarelli, "A meta-active learning approach exploiting instance importance," *Expert Systems with Applications*, vol. 247, p. 123320, Aug. 2024. [Online]. Available: <https://www.sciencedirect.com/science/article/pii/S0957417424001854>

[39] Y. J. Cho, J. Wang, and G. Joshi, "Towards understanding biased client selection in federated learning," in Proceedings of The 25th International Conference on Artificial Intelligence and Statistics. PMLR, May 2022, pp. 10351–10375, ISSN: 2640-3498. [Online]. Available: <https://proceedings.mlr.press/v151/jee-cho22a.html>

[40] I. Loschilov and F. Hutter, "Sgdr: Stochastic gradient descent with warm restarts," 2016. [Online]. Available: <https://arxiv.org/abs/1608.03983>

[41] A. Krizhevsky, V. Alex, and G. Hinton, "CIFAR-10 and CIFAR-100 datasets," 2009. [Online]. Available: <https://www.cs.toronto.edu/~kriz/cifar.html>

[42] P. Wagner, N. Strothoff, R.-D. Bousseljot, W. Samek, and T. Schaeffter, "PTB-XL, a large publicly available electrocardiography dataset," 2020. [Online]. Available: <https://physionet.org/content/ptb-xl/1.0.3/>

[43] Y. Chen, Y. Hao, T. Rakthanmanon, J. Zakaria, B. Hu, and E. Keogh, "A general framework for never-ending learning from time series streams," *Data Mining and Knowledge Discovery*, vol. 29, no. 6, pp. 1622–1664, Nov. 2015. [Online]. Available: <https://doi.org/10.1007/s10618-014-0388-4>

[44] N. Strothoff, P. Wagner, T. Schaeffter, and W. Samek, "Deep learning for ecg analysis: Benchmarks and insights from ptb-xl," *IEEE Journal of Biomedical and Health Informatics*, vol. 25, no. 5, pp. 1519–1528, 2021.

[45] A. Paszke, S. Gross, F. Massa, A. Lerer, J. Bradbury, G. Chanan, T. Killeen, Z. Lin, N. Gimelshein, L. Antiga, A. Desmaison, A. Kopf, E. Yang, Z. DeVito, M. Raison, A. Tejani, S. Chilamkurthy, B. Steiner, L. Fang, J. Bai, and S. Chintala, "Pytorch: An imperative style, high-performance deep learning library," in *Advances in Neural Information Processing Systems 32*. Curran Associates, Inc., 2019, pp. 8024–8035. [Online]. Available: <http://papers.neurips.cc/paper/9015-pytorch-an-imperative-style-high-performance-deep-learning-library.pdf>

[46] T. Danka and P. Horvath, "modAL: A modular active learning framework for Python," available on arXiv at <https://arxiv.org/abs/1805.00979>. [Online]. Available: <https://github.com/cosmic-cortex/modAL>

[47] V. Kaushal, G. Ramakrishnan, and R. Iyer, "Submodlib: A submodular optimization library," Feb. 2022. [Online]. Available: <http://arxiv.org/abs/2202.10680>

[48] A. Kirsch and Y. Gal, "Unifying approaches in active learning and active sampling via fisher information and information-theoretic quantities," Jan. 2022, publisher: arXiv Version Number: 2. [Online]. Available: <https://arxiv.org/abs/2208.00549>